Nonrelativistic QCD factorization and the velocity dependence of NNLO poles in heavy quarkonium production

Gouranga C. Nayak,[1] Jian-Wei Qiu,[2] and George Sterman[1]

[1]*C. N. Yang Institute for Theoretical Physics, Stony Brook University, Stony Brook, New York 11794-3840, USA*
[2]*Department of Physics and Astronomy, Iowa State University, Ames, Iowa 50011, USA*

(Received 8 August 2006; published 12 October 2006)

We study the transition of a heavy quark pair from octet to singlet color configurations at next-to-next-to-leading order in heavy quarkonium production. We show that the infrared singularities in this process are consistent with nonrelativistic QCD factorization to all orders in the heavy quark relative velocity v. This factorization requires the gauge-completed matrix elements that we introduced previously to prove next-to-next-to-leading-order factorization to order v^2.

DOI: 10.1103/PhysRevD.74.074007 PACS numbers: 12.38.Bx, 12.39.St, 13.87.Fh, 14.40.Gx

I. INTRODUCTION

Heavy quarkonium production serves as a testing ground for perturbative and effective field theory treatments of QCD, particularly nonrelativistic QCD (NRQCD) [1]. NRQCD, which relies on an expansion in the heavy quark relative velocity, as well as in α_s, has provided compelling explanations for quarkonium production at collider [2] and fixed target experiments [3]. At the same time, puzzles remain, especially from polarization measurements at the Tevatron [4] and associated production at the B factories [5]. Heavy quarkonium production in the evolving QCD medium at the RHIC and CERN LHC [6] may also play a role in the detection and analysis of new states of strongly interacting matter. For recent updates on heavy quarkonium production at zero and finite temperature QCD, see Refs. [7,8].

The application of NRQCD to heavy quarkonium production processes is based on a very specific factorization property [1], for which a complete proof has not yet been developed [8]. With this in mind, we tested the factorization hypothesis at next-to-next-to-leading order (NNLO) in Ref. [9]. We found that, as a necessary condition for factorization, the conventional $\mathcal{O}(v^2)$ octet NRQCD production matrix elements must be redefined by incorporating Wilson lines that make them manifestly gauge invariant. We referred to these as gauge-completed matrix elements.

This result was derived by employing an eikonal approximation for the coupling of soft radiation to the heavy quarks. To order v^2, this approximation is adequate to treat the lowest-order electric dipole transitions [10] that transform an octet pair to a singlet, without modifying the spin. In this paper, we extend our eikonal NNLO analysis, and show that the factorization of such transitions can be extended from order v^2 to finite v, that is, to all orders in the relative velocity, in terms of gauge-completed NRQCD matrix elements. The essential result is that, at all orders in v, the infrared divergence at NNLO is independent of the direction of the lightlike Wilson line that renders the matrix element gauge invariant. We find this result intriguing, and while this modest extension of our previous result does not address the behavior of spin-dependent operators, it should encourage further work on the factorization theorem.

In the following section we review the role of gauge-completed matrix elements in NRQCD factorization, and the requirements that factorization places on these matrix elements and the infrared poles in dimensional regularization that they must match. We also introduce the specific NNLO eikonal factor that we will calculate to test factorization at this order, and give the result of our calculations. The details of our NNLO calculation are presented in Sec. III, where we verify that the necessary conditions for NRQCD factorization are met to all powers in the relative velocity, after which we give a brief conclusion.

II. INFRARED POLES AND NRQCD FACTORIZATION

In NRQCD, the production cross section for heavy quarkonium H at transverse momentum p_T factorizes into a sum of perturbative functions times universal matrix elements,

$$d\sigma_{A+B\to H+X}(p_T) = \sum_n d\hat{\sigma}_{A+B\to c\bar{c}[n]+X}(p_T)\langle\mathcal{O}_n^H\rangle, \qquad (1)$$

where each matrix element $\langle\mathcal{O}_n^H\rangle$ represents the probability for a heavy quark pair in state $[n]$ to produce quarkonium state H. The states n may, in particular, be color octet or singlet.

Correspondingly, at large p_T, the fragmentation function for parton i to evolve into a heavy quarkonium is factorized according to [10]

$$D_{H/i}(z, m_c, \mu) = \sum_n d_{i\to c\bar{c}[n]}(z, m_c, \mu)\langle\mathcal{O}_n^H\rangle, \qquad (2)$$

in terms of the same matrix elements, along with perturbative functions $d_{i\to c\bar{c}[n]}(z, m_c, \mu)$ that describe the evolution of an off-shell parton into a quark pair in state $[n]$, including logarithms of μ/m_c.

Although we cannot compute the full fragmentation function in perturbation theory, for NRQCD factorization to hold we must be able to compute the function $d_{i\to c\bar{c}[n]}(z, m_c, \mu)$ in Eq. (2) systematically. To do this, we must be able to use regularized perturbation theory to compute probabilities for the production of a singlet quark pair from any local source, and match the infrared singularities of these probabilities to the matrix elements in the sum over n in Eq. (1) and/or Eq. (2).

A. Gauge-completed matrix elements

As advocated in [9], it is natural to define gauge-invariant octet NRQCD operators $\mathcal{O}_n^H$, of the general form

$$\langle \mathcal{O}_n^H(0)\rangle = \langle 0|\chi^\dagger(0)\kappa_{n,e}\psi(0)\Phi_l^{(A)\dagger}(0)_{eb} \times (a_H^\dagger a_H)\Phi_l^{(A)}(0)_{ba}\psi^\dagger(0)\kappa'_{n,a}\chi(0)|0\rangle, \quad (3)$$

in terms of heavy quark (ψ) and antiquark (χ) operators, and local combinations of color and spin matrices and/or covariant derivatives, denoted by $\kappa_{n,e}$ and $\kappa'_{n,a}$. The operator $a_H^\dagger$ creates quarkonium H, and the operators $\Phi_l^{(A)}(0)$ are Wilson lines, that is, ordered exponentials, constructed from the gauge field in adjoint matrix representation, $A_\mu^{(A)}$, as

$$\Phi_l^{(A)}(0) = \mathcal{P}\exp\left[-ig\int_0^\infty d\lambda l\cdot A^{(A)}(l\lambda)\right], \quad (4)$$

where $\mathcal{P}$ denotes path ordering and l^μ is the velocity of the source. In (complex conjugate) amplitudes, (anti)time-ordering is understood.

For NRQCD factorization to hold, a necessary, and superficially paradoxical, property of the gauge-completed matrix elements is that their long-distance behavior must be independent of the vector l^μ that we choose to define them [9]. Such a dependence would be inconsistent with NRQCD factorization, because the infrared divergences of $\mathcal{O}_n^H$ must match those of cross sections, in which there is no information on l^μ. In Ref. [9], we have verified the l-independence of the infrared pole to order v^2 in the relative velocity of the pair, at order NNLO. We will extend this result below to all powers in v, again at NNLO.

B. Matrix elements and infrared universality

In this paper, we will study the infrared behavior of the octet, S-wave matrix elements

$$\mathcal{M}^{(8\to I)}(P_1, P_2, l) = \sum_X \langle 0|\chi^\dagger(0)T_e^{(q)}\psi(0)\Phi_l^{(A)\dagger}(0)_{eb}|[c(P_1)\bar{c}(P_2)]^{(I)}X\rangle \times \langle X[c(P_1)\bar{c}(P_2)]^{(I)}|\Phi_l^{(A)}(0)_{ba}\psi^\dagger(0)T_a^{(q)}\chi(0)|0\rangle, \quad (5)$$

where $I = 1, 8$ labels the color of the heavy quark pair, with momenta P_1 and P_2. The $T_i^{(q)}$ are color generators in the quark fundamental representation. We will compute the infrared poles of Eq. (5) to NNLO. At lowest order, of course, only $I = 8$ contributes in the final state. At higher orders, however, the octet state mixes with the singlet state, through radiation to states X. The phase space of X is cut off at a UV scale μ, which we take to be of the order of the heavy quark mass.

In Eq. (5), we specify the pair's momenta in a conventional fashion, in terms of the total pair (P) and relative momentum (q), and center-of-mass velocity (v) by

$$P_1 = \frac{P}{2} + q, \qquad P_2 = \frac{P}{2} - q, \qquad v^2 = \frac{\vec{q}^2}{E^{*2}}, \quad (6)$$

where $2E^*$ is the total center-of-mass energy of the pair in the pair's rest frame. We note that our convention for the relative velocity here differs from the one in our previous study, Ref. [9], where we defined the relative velocity as $2\vec{q}/m$, with m the heavy quark mass.

NRQCD requires that, when we expand $\mathcal{M}$ of Eq. (5) in powers of q in perturbation theory, we should find infrared-finite coefficient functions times infrared-sensitive but universal NRQCD matrix elements,

$$\mathcal{M}^{(8\to I)}(P_1, P_2, l) = \sum_n \hat{\mathcal{C}}_n^{(8)}(P_1, P_2, l)\langle \mathcal{O}_n^I\rangle, \quad (7)$$

where $\hat{\mathcal{C}}_n^{(8)}$ is a perturbative coefficient function for NRQCD operator $\mathcal{O}_n^I$ with the sum over all operators n for a given final state in which the heavy quark pair has color I. To test these ideas, we must study the infrared behavior of such a matrix element when the color of the final state is fixed as a singlet, $I = 1$.

The formation of a heavy quarkonium state, of course, cannot be realized to any fixed order of perturbation theory. Nevertheless, the factorization expressed in Eqs. (1), (2), and (7) is useful to the extent that we can systematically compute corrections to short-distance functions in each case. This, in turn, requires that the infrared poles encountered in the evolution of the heavy quark pair from octet to singlet in $\langle \mathcal{O}_n^H\rangle$ in Eq. (2) match those of cross sections for the production of a singlet quark pair. As already noted, a necessary condition for this matching is that the poles in the matrix element should not depend on the direction of the vector l^μ that is introduced in gauge completion of the matrix elements, Eq. (3), since the choice of l^μ is a matter of convention.

Now we are ready to describe the NNLO calculation that tests these ideas. A full NNLO calculation of $\mathcal{M}^{(8\to 1)}$ in Eq. (5) would be impractical, but its infrared singularities are easier to compute. These divergences can be generated by a factorization that is much simpler than Eq. (7), and which can be carried out at fixed momenta P_1 and P_2,

$$\mathcal{M}^{(8\to 1)}(P_1, P_2, l) = \sum_J \mathcal{C}_{8J}(P_1, P_2, l)\mathcal{E}^{(J\to 1)}(P_1, P_2, \varepsilon). \quad (8)$$

All spin information in $\mathcal{M}^{(8\to1)}$ is contained in another short-distance function $\mathcal{C}_{8J}$, which describes a transition of octet to color configuration J at short distances. Although $\mathcal{C}_{8J}$ may depend on l^μ, it must be finite for $\varepsilon \to 0$. All $1/\varepsilon$ poles are absorbed into an infrared factor, $\mathcal{E}^{(8\to1)}$, whose pole structure, however, must be independent of l^μ. The expansion of the infrared factor, $\mathcal{E}^{(J\to1)}(P_1, P_2, \varepsilon)$, in the relative velocity, v, of the pair should lead us back to a set of l-independent operator matrix elements for producing a color-singlet quark pair ($I = 1$) in Eq. (7). The essential result of this paper is that at NNLO the infrared poles of the function $\mathcal{E}^{(8\to1)}(P_1, P_2, \varepsilon)$ are indeed independent of the vector l, for arbitrary v. This generalizes the result of Ref. [9] from v^2 "electric dipole" transitions to arbitrary powers of v at NNLO.

Specifically, we will find an explicit single-pole contribution, which can be written as a prefactor determined by N_c (the number of colors) times a function that depends only on the relative velocity,

$$\mathcal{E}^{(8\to1)}(P_1, P_2, \varepsilon) = -\frac{N_c}{4}(N_c^2 - 1)\mathcal{I}^{8\to1}(v, \varepsilon). \quad (9)$$

The velocity-dependent factor $\mathcal{I}^{8\to1}(v, \varepsilon)$ is given by

$$\mathcal{I}^{(8\to1)}(v, \varepsilon) = \frac{\alpha_s^2}{4\varepsilon}\left\{1 - \frac{1}{2f(|\vec{v}|)}\ln\left[\frac{1 + f(|\vec{v}|)}{1 - f(|\vec{v}|)}\right]\right\}, \quad (10)$$

where $v = |\vec{v}|$ is the relative velocity of the quark and antiquark in the pair center of mass, and where $f(v) = 2v/(1 + v^2)$. As anticipated, $\mathcal{I}^{8\to1}(v, \varepsilon)$ is independent of l. We will compute the color factor given in Eq. (9) below. To derive the result of Eq. (10), we will first recall the use of the eikonal approximation to isolate infrared behavior.

C. Soft gluon interactions

The eikonal approximation reproduces all infrared divergences in the evolution of the pair into the final state, and it must be defined by an infrared regularization. We will use a continuation to $4 - 2\varepsilon$ dimensions, with $\varepsilon < 0$.

The eikonal approximation for the interactions of the heavy quarks with soft gluons is generated by ordered exponentials, this time in fundamental representations and in the directions of the heavy quark and antiquark momenta. The perturbation theory rules for the ordered exponentials are equivalent to the eikonal approximation. Eikonal quark propagators and gluon-quark vertices are specified, respectively, by

$$\frac{i}{(\beta\cdot k + i\epsilon)}, \qquad \pm i g_s T_a^{(q)}\beta^\mu, \quad (11)$$

where the plus is for the antiquark and the minus for the quark vertices, and where β^μ is a timelike four-velocity. Because the product of an eikonal propagator and vertex is always scale invariant, we will use below the momenta defined in Eq. (6) for the eikonal velocities of the quark pair.

The long-distance evolution of the pair from octet to singlet color configurations is given by the infrared factor $\mathcal{E}^{(8\to1)}$ of Eq. (8), which can be represented as a matrix element. This matrix element is given in the notation of Eq. (5) by

$$\begin{aligned}\mathcal{E}^{(8\to1)}(P_1, P_2, \varepsilon) &= \sum_N \langle 0|[\Phi_{P_2}^{(\bar q)\dagger}(0)]_{IJ}[T_e^{(q)}]_{JK}[\Phi_{P_1}^{(q)\dagger}(0)]_{KI}\Phi_l^{(A)\dagger}(0)_{eb}|N\rangle \\ &\quad\times\langle N|\Phi_l^{(A)}(0)_{ba}[\Phi_{P_1}^{(q)}(0)]_{LM}[T_a^{(q)}]_{MN}[\Phi_{P_2}^{(\bar q)}(0)]_{NL}|0\rangle.\end{aligned} \quad (12)$$

Here we have exhibited all color indices: those in the adjoint representation by $a, b\ldots$, and those in the fundamental representation by $I, J\ldots$, to indicate the trace structure, which imposes a color-singlet configuration on the quark pair in the final state. In Eq. (12) and below, overall time-ordering of the field operators is understood in the amplitude, and anti-time-ordering in its complex conjugate.

The operators $\Phi^{(q)}$ and $\Phi^{(\bar q)}$ are the ordered exponentials that represent the quark and antiquark. The quark (antiquark) ordered exponential has the same (opposite) ordering compared to time-ordering. To be specific, we represent normal (reverse) matrix ordering by $\mathcal{P}$ ($\bar{\mathcal{P}}$), and define

$$\begin{aligned}\Phi_{P_1}^{(q)}(0) &= \mathcal{P}\exp\left[-ig\int_0^\infty d\lambda P_1\cdot A^{(q)}(P_1\lambda)\right], \\ \Phi_{P_2}^{(\bar q)}(0) &= \bar{\mathcal{P}}\exp\left[ig\int_0^\infty d\lambda P_2\cdot A^{(q)}(P_2\lambda)\right].\end{aligned} \quad (13)$$

For classical fields, $\Phi_n^{(\bar q)}(0)$ is the Hermitian conjugate of $\Phi_n^{(q)}(0)$. The matrix $A_\nu^{(q)} \equiv \sum_a T_a^{(q)}A_{\nu,a}$ is the gauge field operator in the quark fundamental representation.

The matrix element in Eq. (12) is equal to unity when $q = 0$. In Ref. [9] we expanded Eq. (12) to second order in q, and found an expression in terms of field strength operators,

$$\begin{aligned}\mathcal{E}_2^{(8\to1)}(p + q, p - q, \varepsilon) \equiv \sum_N \int_0^\infty d\lambda'\lambda'\langle 0|\Phi_l^{(A)\dagger}(0)_{bd'} \\ \times\Phi_p^{(A)}(\lambda')^\dagger_{d'a'}[p^\mu q^\nu F_{\nu\mu,a'}(\lambda' p)]|N\rangle \\ \times\int_0^\infty d\lambda\lambda\langle N|\Phi_l^{(A)}(0)_{bd} \\ \times[p^\mu q^\nu F_{\nu\mu,a}(\lambda p)]\Phi_p^{(A)}(\lambda)_{ad}|0\rangle.\end{aligned} \quad (14)$$

In this expression, the momenta p^μ and q^μ are taken to be dimensionless, scaled by the heavy quark mass m. We notice that in the heavy quark rest frame, $p \equiv (1/2m)\times(P_1 + P_2)_{\rm rest} = \delta_{\mu0}$, the relevant operator is precisely the

chromo-electric field $F_{\mu 0}$, and the matrix elements describe an electric dipole transition.

The basic result of Ref. [9] was to identify an infrared pole in $\mathcal{E}_2^{(8\to 1)}$, associated with the exchange of gluons between the heavy quark pair and the eikonal source Φ_l. The presence of such a pole showed first that the infrared behavior of the fragmentation function is not summarized by ''topologically factorized'' diagrams alone in an arbitrary gauge [10]. The specific form, however, depends on the relative velocity of the pair only. In terms of the center-of-mass velocity of the heavy quark and antiquark, defined as in Eq. (6) above, the result is[1]

$$\mathcal{E}_2^{(8\to 1)}(v) = \frac{N_c}{4}(N_c^2-1)\alpha_s^2\frac{1}{3\varepsilon}v^2. \tag{15}$$

The prefactor here is the same color factor given in Eq. (9) above. The crucial point is that the pole due to topologically nonfactored diagrams is independent of the direction of the lightlike vector l^μ. In Ref. [9] we showed that this implies that the gauge completion of the NRQCD matrix element is adequate to match this infrared structure in production processes with arbitrary numbers of recoiling jets. This verified the NRQCD factorization of Eq. (2) at NNLO in soft gluon corrections for octet operators. We will show here that this result generalizes to all orders in v for the full infrared factor $\mathcal{E}^{(8\to 1)}$.

In our calculation below, we will keep q, or equivalently the relative velocity v, finite and nonzero, and evaluate Eq. (12) directly to NNLO (α_s^2), without an expansion in velocity. Restricting ourselves to this order in α_s, an expansion in v will be describable at any order in terms of derivatives of the electric field strength. In this sense our calculation identifies the infrared pole in the sum of electric multipole transitions generated by NNLO. Because of the eikonal approximation, no information on spin dependence is included in the calculation, and the consequences for matching are similar to the v^2 case. We will once again find an infrared pole to any order in v^2, and we will once again find that the pole is independent of the direction of the vector l^μ. This surprising result shows that matching to gauge-completed NRQCD matrix elements is not limited to lowest order in v^2 but, to this order in α_s and for this class of electric dipole transitions, is true to all orders in the relative velocity v.

III. FINITE-v DIAGRAMS

A. Ladder and three-gluon diagrams

Our goal is to calculate the noncanceling infrared pole term in Eq. (12), the eikonal infrared factor at finite relative velocity v. As in Ref. [9], we need only consider diagrams

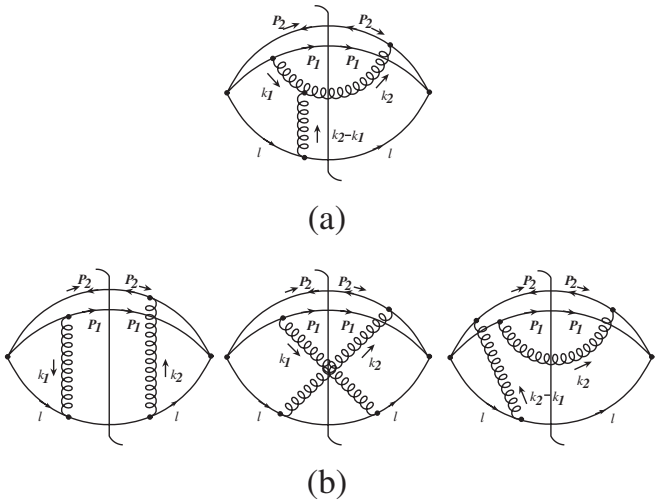

FIG. 1. Examples of NNLO diagrams for quarkonium production. (a) Three-gluon diagram, (b) QED-like diagrams. The projection of the quark pair onto a color singlet in the final state is understood.

that are not topologically factorized. As indicated above, we take the quark momentum as P_1, the antiquark as P_2, and the momentum of the gauge line as l, with $l^2 = 0$. The gauge line may be thought of as part of a fragmentation function, or as representing an approximation to a recoiling jet in a hard-scattering cross section.

The relevant diagrams are illustrated in Fig. 1, with quark-antiquark eikonal lines on top, and the gluon eikonal below. In each case, the vertical line indicates the color-singlet heavy quark pair, and the sum over other possible final states is understood. The left- and right-most vertices in each diagram couple the lightlike color octet eikonal on the bottom of the diagram with the color octet projection of the eikonals on the top that represent the heavy quark pair, in the fundamental representations.

The quark lines radiate soft gluons to transform themselves from color octet to color singlet, as in the classic description of the color octet mechanism. At NNLO, however, these soft gluons can scatter from the eikonal gluon in the l direction. To this order, the diagrams either contain the three-gluon coupling as in Fig. 1(a), or are QED-like as in Fig. 1(b). Of these, only the former gives rise to noncanceling infrared poles, generalizing the result of Ref. [9].[2] The color factor in Eq. (10) is thus found entirely from Fig. 1(a). This factor is the product of two simple traces in the fundamental representation, and the color tensors from two three-gluon vertices,

$$\begin{aligned} F_{\text{color}} &= \mathrm{Tr}[T_e^{(q)}T_g^{(q)}]\,\mathrm{Tr}[T_a^{(q)}T_h^{(q)}]f_{eai}f_{ihg}, \\ &= -\frac{N_c}{4}(N_c^2-1). \end{aligned} \tag{16}$$

[1]The coefficient of v^2 here is 4 times larger than in Ref. [9], where the velocity was defined by $2\vec{q}/m$, as noted in connection with Eq. (6) above.

[2]It is worth noting that the color factor of the left-most diagram in Fig. 1(b) vanishes in the matrix element of Eq. (12).

The two traces reflect the projection of the quark-antiquark eikonal pair onto the singlet in the final state that is built into the matrix element of Eq. (12). In the traces, one generator is associated with the operator in the corresponding matrix element and the other with the corresponding quark-gluon vertex shown in Fig. 1(a). We now turn to the calculation of the velocity dependence of $\mathcal{E}^{(8\to1)}$.

B. Velocity dependence of $\mathcal{E}^{(8\to1)}$

We will give a detailed discussion of the cut diagrams illustrated in Fig. 2(a). In these four cut diagrams, a soft gluon is emitted by one member of the (eikonal) heavy quark pair in the amplitude and is absorbed by one in the complex conjugate amplitude. This soft gluon rescatters from the spectator eikonal gluon of momentum l in either the amplitude or the complex conjugate. For each of these diagrams the leading order v^2 expansion of this contribution to $\mathcal{E}_2$, Eq. (14), was calculated in detail in Ref. [9] (where it was referred to as diagram IIIA). Here we extend this calculation to all orders in v by directly calculating the full velocity dependence of $\mathcal{E}^{(8\to1)}$.

All of the diagrams in Fig. 2 have the same color factor [the same as in Eq. (16) above] when the quark pair is projected onto a color singlet in the final state. We will suppress the common color factor in our calculation below, and denote the sum of the relevant NNLO diagrams as $\mathcal{I}^{(8\to1)} = \mathcal{E}^{(8\to1)}/F_{\rm color}$. We label the diagrams of Fig. 2, whose sum gives $\mathcal{I}^{(8\to1)}$, by

$$\mathcal{I}^{(8\to1)}(P,q,l) = 2\,\mathrm{Re}\Big[\sum_{i,j=1,2}\mathcal{I}^{P_iP_j}(P,q,l)\Big], \tag{17}$$

where the first superscript, P_i, on the right identifies the gluon coupling in the amplitude to the quark, P_1, or antiquark, P_2, and the second, P_j, identifies the gluon coupling in the complex conjugate. As in Ref. [9], we fix the momentum of the eikonal l in the minus light cone direction,

$$l^\mu = \delta_{\mu-}. \tag{18}$$

The momenta P_1 and P_2 remain arbitrary. We have used the scale invariance of the eikonal diagrams to set l^- to unity.

1. The P_1P_1 gluon rescattering diagram

We begin with the diagram $\mathcal{I}^{P_1P_1}$, Fig. 2(a), which describes the interference between the order g_s^3 rescattering of a gluon that is emitted by the heavy quark (P_1) eikonal line and the lowest-order process in which it is emitted by the same line.

Written out with the momentum structure of the eikonal vertices in Eq. (11) shown explicitly, this diagram is given by

$$\begin{aligned}\mathcal{I}^{P_1P_1}(P,q,l) = \int \frac{d^Dk_1}{(2\pi)^D}\frac{d^Dk_2}{(2\pi)^D}2\pi\delta(k_2^2)\\ \times\frac{-i}{[(k_2-k_1)^2+i\epsilon]}\frac{-i}{[k_1^2+i\epsilon]}\\ \times(-g\mu^\varepsilon V_{\nu,\mu,\lambda}[k_1,k_2-k_1,-k_2])\\ \times\frac{i(-ig\mu^\varepsilon)P_1^\nu}{[P_1\cdot k_1+i\epsilon]}\frac{-i(ig\mu^\varepsilon)P_1^\lambda}{[P_1\cdot k_2-i\epsilon]}\\ \times\frac{-i(-g\mu^\varepsilon l^\mu)}{[l\cdot(k_2-k_1)+i\epsilon]},\end{aligned} \tag{19}$$

where the three-gluon vertex (with all momenta flowing in) is

$$\begin{aligned}V_{\mu_1,\mu_2,\mu_3}[q_1,q_2,q_3] = (q_1-q_2)_{\mu_3}g_{\mu_1\mu_2} + (q_2-q_3)_{\mu_1}g_{\mu_2\mu_3}\\ + (q_3-q_1)_{\mu_2}g_{\mu_3\mu_1}.\end{aligned} \tag{20}$$

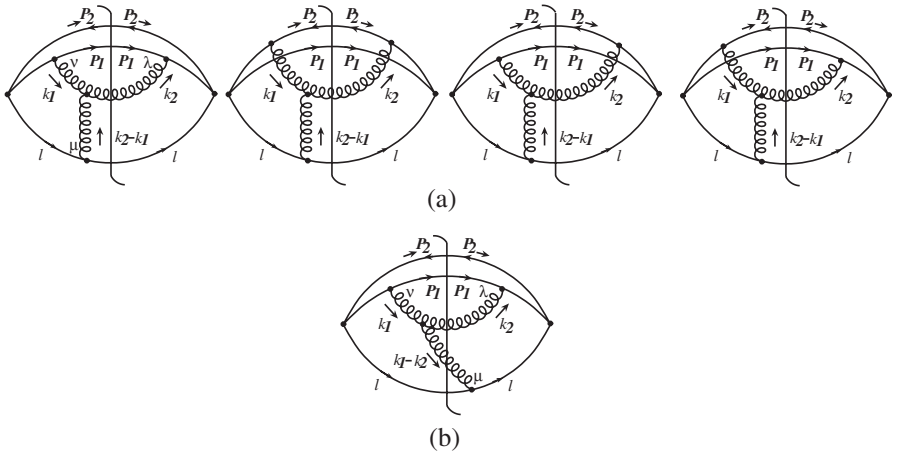

FIG. 2. (a) The four relevant cut diagrams with three-gluon vertices. The P_1, P_2, and l lines are eikonal. The full contribution of each diagram to $\mathcal{I}^{(8\to1)}$ is found by summing over other cuts that include the singlet pair. (b) An example of a two-gluon final state that cancels the $(k_2-k_1)^2=0$ pole, as discussed in the text. As in Fig. 1, the projection of the quark pair onto a color singlet in the final state is understood.

As in Eq. (6), P and q are the total and relative momenta of the pair. As in $\mathcal{I}^{(8\to 1)}$, Eq. (12), P_1 and P_2 are the momenta of the heavy quark and antiquark, respectively, and l is the momentum of the lightlike eikonal. As indicated in the diagram, we take k_1 as the momentum of the soft gluon emitted in the amplitude, to the left of the cut in Fig. 2, and k_2 as the momentum of the soft gluon flowing to the right in the figure.[3]

Following the procedure of Ref. [9], we find it useful to integrate first the minus components of k_1 and k_2. Performing the k_2^- integration by using the mass-shell delta function, and evaluating the numerator factors, we find

$$\mathcal{I}^{P_1P_1}(P,q,l) = i\frac{g^4\mu^{4\varepsilon}}{(2\pi)^{2D-1}}\int_{-\infty}^{\infty} d^{D-2}k_1^T \int_{-\infty}^{\infty} dk_1^+ \int_{-\infty}^{\infty} dk_1^- \int_{k_2^T<\mu} d^{D-2}k_2^T \int_0^{\mu}\frac{dk_2^+}{2k_2^+}\Bigg[\Bigg(P_1^+\Bigg(\frac{k_2^{T2}}{2k_2^+}+k_1^-\Bigg)+P_1^-(k_2^+ + k_1^+) - P_1^T\cdot(k_2^T+k_1^T)\Bigg) - \frac{P_1^2}{P_1^+}(k_2^+ + k_1^+)\Bigg]\frac{1}{[k_2^+ - k_1^+ + i\epsilon]}\frac{1}{[\frac{P_1^+k_2^{T2}}{2k_2^+}+P_1^-k_2^+ - P_1^T\cdot k_2^T - i\epsilon]} \times\frac{1}{[2(k_1^+ - k_2^+)(k_1^- - \frac{k_2^{T2}}{2k_2^+}) - (k_1^T - k_2^T)^2 + i\epsilon]}\frac{1}{[2k_1^+k_1^- - k_1^{T2} + i\epsilon]}\frac{1}{[k_1^- + \frac{P_1^-k_1^+}{P_1^+} - \frac{P_1^T\cdot k_1^T}{P_1^+} + i\epsilon]}. \tag{21}$$

Below we will generally suppress limits on the loop (k_1) and real-gluon momentum (k_2) integrals, except where they are necessary for the argument. The k_1 integrals are unbounded, while the k_2 integrals are understood to be cut off at the order of the quark mass. These upper limits are set by the phase space cutoff, denoted μ here, and discussed above in connection with the basic matrix element of Eq. (5).

The next step is the loop integral k_1^- in Eq. (21), which we perform by contour integration. The integrand of (21) has three poles in k_1^-,

$$\begin{aligned} k^-_{1[k_1^2]} &= \frac{k_1^{T2} - i\epsilon}{2k_1^+}, \\ k^-_{1[(k_1-k_2)^2]} &= \frac{k_2^{T2}}{2k_2^+} + \frac{(k_1^T - k_2^T)^2 - i\epsilon}{2(k_1^+ - k_2^+)}, \\ k^-_{1[P_1\cdot k_1]} &= \frac{P_1^T\cdot k_1^T}{P_1^+} - \frac{P_1^-k_1^+}{P_1^+} - i\epsilon, \end{aligned} \tag{22}$$

labeled according to the denominator that vanishes.

The pattern of poles encountered here is similar to those for the order-v^2 calculation of Ref. [9], and the role of each term is similar. When we close the k_1^- contour in the lower half-plane, we pick up the $k^-_{1[k_1^2]}$ pole when $k_1^+ > 0$, the $k^-_{1[(k_1-k_2)^2]}$ pole when $k_1^+ > k_2^+$, and the $k^-_{1[p_1\cdot k_1]}$ pole for all values of k_1^+. The contribution from the $k^-_{1[k_1^2]}$ pole vanishes, because the resulting integral is antisymmetric under the exchange of the remaining components of k_1 and k_2. The $k^-_{1[(k_1-k_2)^2]}$ contribution, on the other hand, cancels against the corresponding cut in which the gluon with momentum $k_1 - k_2$ appears in the final state, as in Fig. 2(b).

This leaves us with the third, $k^-_{1[P_1\cdot k_1]}$, pole only, whose calculation we describe in detail below for $\mathcal{I}^{P_1P_1}(P,q,l)$ and $\mathcal{I}^{P_1P_2}(P,q,l)$. We note that, in the sum of $\mathcal{I}^{P_1P_2}(P,q,l)$ and $\mathcal{I}^{P_2P_1}(P,q,l)$, the symmetry argument for the cancellation of the $k^-_{1[k_1^2]}$ pole continues to apply.

In summary, to derive the infrared contribution to $\mathcal{I}^{P_1P_1}(P,q,l)$ from Fig. 2, we close the k_1^- integration in Eq. (21) in the lower half-plane at the pole $k^-_{1[P_1\cdot k_1]}$, and find

$$\mathcal{I}^{P_1P_1}(P,q,l) = (-2\pi i)(i)\frac{g^4\mu^{4\varepsilon}}{(2\pi)^{2D-1}}\int d^{D-2}k_1^T\int dk_1^+\int d^{D-2}k_2^T\int\frac{dk_2^+}{2k_2^+}\Bigg[P_1^+\Bigg(\frac{k_2^{T2}}{2k_2^+}+\Bigg(\frac{P_1^T\cdot k_1^T}{P_1^+}-\frac{P_1^-k_1^+}{P_1^+}\Bigg)\Bigg) + P_1^-(k_2^+ + k_1^+) - P_1^T\cdot(k_2^T+k_1^T) - \frac{P_1^2}{P_1^+}(k_2^+ + k_1^+)\Bigg]\frac{-1}{[k_1^+ - k_2^+ - i\epsilon]}\frac{1}{[\frac{P_1^+k_2^{T2}}{2k_2^+}+P_1^-k_2^+ - P_1^T\cdot k_2^T - i\epsilon]} \times\frac{1}{[2(k_1^+ - k_2^+)((\frac{P_1^T\cdot k_1^T}{P_1^+}-\frac{P_1^-k_1^+}{P_1^+}) - \frac{k_2^{T2}}{2k_2^+}) - (k_1^T - k_2^T)^2 + i\epsilon]}\frac{1}{[2k_1^+(\frac{P_1^T\cdot k_1^T}{P_1^+}-\frac{P_1^-k_1^+}{P_1^+}) - k_1^{T2} + i\epsilon]}. \tag{23}$$

In this expression we have two (D-2 dimensional) transverse and two plus integrals remaining. We begin by applying a Feynman parametrization to the final two denominators,

[3]In the discussion that follows, we will compute diagrams with loops in the amplitude, in contrast to the complex conjugate amplitude as in Ref. [9]. Since our result is real, the analysis is otherwise completely equivalent.

$$\mathcal{I}^{P_1P_1}(P,q,l) = -\frac{g^4\mu^{4\varepsilon}}{(2\pi)^{2D-2}}\int_0^1 dx\int d^{D-2}k_2^T\int dk_1^+\int\frac{dk_2^+}{2k_2^+}\int d^{D-2}k_1'^T\Big[P_1^+\Big(\frac{k_2^{T2}}{2k_2^+}+\Big(\frac{P_1^T\cdot(k_1'^T+K^T(P_1))}{P_1^+}-\frac{P_1^-k_1^+}{P_1^+}\Big)\Big)$$
$$+P_1^-(k_2^++k_1^+)-P_1^T\cdot(k_2^T+k_1'^T+K^T(P_1))-\frac{P_1^2}{P_1^+}(k_2^++k_1^+)\Big]$$
$$\times\frac{1}{[k_1^+-k_2^+-i\epsilon]}\frac{1}{[\frac{P_1^+k_2^{T2}}{2k_2^+}+P_1^-k_2^+-P_1^T\cdot k_2^T-i\epsilon]}\frac{1}{[k_1'^{T2}+L(P_1)-i\epsilon]^2}, \tag{24}$$

where to complete the square we have shifted to $k_1'^T = k_1^T - K^T(P_1)$, with

$$K^T(P_1)\equiv x\Big(k_2^T+\frac{(k_1^+-k_2^+)}{P_1^+}P_1^T\Big)+(1-x)\frac{k_1^+}{P_1^+}P_1^T. \tag{25}$$

In addition, in the final denominator of (24) we introduce the function

$$L(P_1)\equiv x\Big[\frac{k_1^+}{k_2^+}-x\Big]\Big[\Big(k_2^T-\frac{k_2^+}{P_1^+}P_1^T\Big)^2+\frac{k_2^+k_1^+}{xP_1^{+2}}P_1^2\Big]. \tag{26}$$

Here and below, to simplify the notation we suppress the k_1 and k_2 dependence in $L(P_1)$ and $K^T(P_1)$.

We now perform the $k_1'^T$ integration of Eq. (24) in $D = 4-2\varepsilon$ dimensions, obtaining

$$\mathcal{I}^{P_1P_1}(P,q,l) = -\pi^{1-\varepsilon}\Gamma(1+\varepsilon)\frac{g^4\mu^{4\varepsilon}}{(2\pi)^{2D-2}}\int_0^1 dx\int dk_1^+\int d^{D-2}k_2^T\int\frac{dk_2^+}{2k_2^+}\Big[\Big(P_1^+\frac{k_2^{T2}}{2k_2^+}+P_1^-k_2^+-P_1^T\cdot k_2^T\Big)$$
$$-\frac{P_1^2}{P_1^+}(k_2^++k_1^+)\Big]\frac{1}{[k_1^+-k_2^+-i\epsilon]}\frac{1}{[\frac{P_1^+k_2^{T2}}{2k_2^+}+P_1^-k_2^+-P_1^T\cdot k_2^T-i\epsilon]}\frac{1}{[L(P_1)-i\epsilon]^{1+\varepsilon}}. \tag{27}$$

Simplifying this expression algebraically, we put it into a form that will facilitate the combination of diagrams below,

$$\mathcal{I}^{P_1P_1}(P,q,l) = -\pi^{1-\varepsilon}\Gamma(1+\varepsilon)\frac{g^4\mu^{4\varepsilon}}{(2\pi)^{2D-2}}\int_0^1 dx\int d^{D-2}k_2^T\int\frac{dk_2^+}{2k_2^+}\int dk_1^+\frac{1}{[k_1^+-k_2^+-i\epsilon]}\frac{1}{[L(P_1)-i\epsilon]^{1+\varepsilon}}$$
$$\times\Big[1-\frac{\frac{P_1^2}{P_1^+}(k_2^++k_1^+)}{\frac{P_1^+k_2^{T2}}{2k_2^+}+P_1^-k_2^+-P_1^T\cdot k_2^T-i\epsilon}\Big]. \tag{28}$$

Of particular interest in this expression is the first term, 1, in square brackets. This term has up to four poles in dimensional regularization, corresponding to momentum configurations in which both momenta k_1 and k_2 vanish and are collinear to the lightlike eikonal line l in Fig. 2. We will see that, as in Ref. [9], these singularities cancel, leaving only a single real $1/\varepsilon$ (and imaginary $1/\varepsilon^2$) pole in dimensional regularization.

2. The P_1P_2 diagram and collinear cancellation

Before continuing with the integrals, we turn our attention to the third diagram in Fig. 2(a), which describes interference between gluon (k_1) rescattering after emission from the heavy quark (P_1) line in the amplitude with gluon (k_2) emission from the antiquark (P_2) line in the complex conjugate amplitude. We denote this diagram by $\mathcal{I}^{P_1P_2}(P,q,l)$.

The momentum-space integral for the P_1P_2 rescattering diagram, $\mathcal{I}^{P_1P_2}(P,q,l)$, is

$$\mathcal{I}^{P_1P_2}(P,q,l) = -ig^4\mu^{4\varepsilon}\int\frac{d^Dk_2}{(2\pi)^D}\frac{d^Dk_1}{(2\pi)^D}2\pi\delta(k_2^2)P_1^\nu l^\mu P_2^\lambda V_{\nu,\mu,\lambda}[k_1,k_2-k_1,-k_2]$$
$$\times\frac{1}{[P_1\cdot k_1+i\epsilon][P_2\cdot k_2-i\epsilon][l\cdot(k_2-k_1)+i\epsilon][(k_1-k_2)^2+i\epsilon][k_1^2+i\epsilon]}. \tag{29}$$

The integral $\mathcal{I}^{P_1P_2}$ has an overall (-1) relative to $\mathcal{I}^{P_1P_1}(P,q,l)$, associated with the connection of one gluon to the P_2 eikonal line, which is in the antiquark representation.

Performing on $\mathcal{I}^{P_1P_2}(P,q,l)$ the same steps as above for the k_i^- and k_1^T integrals in $\mathcal{I}^{P_1P_1}(P,q,l)$, we can put this integral into a form analogous to Eq. (28), although slightly more complex,

$$\mathcal{I}^{P_1P_2}(P,q,l) = \pi^{1-\varepsilon}\Gamma(1+\varepsilon)\frac{g^4\mu^{4\varepsilon}}{(2\pi)^{2D-2}}\int_0^1 dx\int d^{D-2}k_2^T\int\frac{dk_2^+}{2k_2^+}\int dk_1^+\frac{1}{[k_1^+-k_2^+-i\epsilon]}\frac{1}{[L(P_1)-i\epsilon]^{1+\varepsilon}}$$
$$\times\left[1-\frac{\frac{P_1\cdot P_2}{P_1^+}(k_1^++k_2^+)+\frac{2}{P_1^+}(k_1^+-k_2^+)(P_2^+P_1^--P_1^+P_2^-)+2P_2^+[\frac{P_2^T}{P_2^+}-\frac{P_1^T}{P_1^+}]\cdot[K^T(P_1)-k_2^T]}{[\frac{P_2^+k_2^{T2}}{2k_2^+}+P_2^-k_2^+-P_2^T\cdot k_2^T-i\epsilon]}\right]. \quad (30)$$

Combining the expressions for $\mathcal{I}^{P_1P_1}(P,q,l)$ and $\mathcal{I}^{P_1P_2}(P,q,l)$, Eqs. (28) and (30), we see that, as anticipated above, the collinear-singular terms (the 1's) in the square brackets cancel.

Our goal now is to evaluate the infrared poles from the expressions in Eqs. (28) and (30). For this purpose we need to perform the k_1^+ integration, which ranges from $-\infty$ to $+\infty$. Noting that the numerators are at most linear in k_1^+, we rewrite factors of k_1^+ in the numerator as $(k_1^+-k_2^+)+k_2^+$. The $(k_1^+-k_2^+)$ term then cancels the corresponding denominator in Eq. (30). We next reorganize the contributions of the P_1P_1 and P_1P_2 diagrams to $\mathcal{I}^{(8\to1)}$ as

$$\mathcal{I}^{P_1P_2}+\mathcal{I}^{P_1P_1} = (\mathcal{J}^{P_1P_2}+\mathcal{J}^{P_1P_1})+(\mathcal{K}^{P_1P_2}+\mathcal{K}^{P_1P_1}), \quad (31)$$

where, for example, $\mathcal{J}^{P_1P_2}$ is obtained from $\mathcal{I}^{P_1P_2}$ by canceling the $(k_1^+-k_2^+)$ factors in the numerator and denominator, and $\mathcal{K}^{P_1P_2}$ represents the remaining terms in $\mathcal{I}^{P_1P_2}$. We now turn to the identification of infrared poles in these expressions, using slightly different procedures in the two cases.

C. The IR pole from the $\mathcal{J}$ terms

We begin with the terms that lack the pole in $k_1^+-k_2^+$. From Eq. (30) we find

$$\mathcal{J}^{P_1P_2}(P,q,l)+\mathcal{J}^{P_1P_1}(P,q,l) = -\pi^{1-\varepsilon}\Gamma(1+\varepsilon)\frac{g^4\mu^{4\varepsilon}}{(2\pi)^{2D-2}}\int_0^1 dx\int dk_2^+\int d^{D-2}k_2^T\int_{-\infty}^{\infty}dk_1^+$$
$$\times\frac{\frac{P_1\cdot P_2}{P_1^+P_2^+}+\frac{2}{P_1^+P_2^+}(P_2^+P_1^--P_1^+P_2^-)+2[\frac{P_2^T}{P_2^+}-\frac{P_1^T}{P_1^+}]\cdot\frac{P_1^T}{P_1^+}}{[L(P_1)-i\epsilon]^{1+\varepsilon}[k_2^{T2}+\frac{P_2^-}{P_2^+}2k_2^{+2}-2k_2^+\frac{P_2^T}{P_2^+}\cdot k_2^T-i\epsilon]}-(P_2\to P_1). \quad (32)$$

In these terms, the remaining (quadratic) k_1^+ dependence is in the $L(P_1)$ denominator. The integral is elementary, and we find

$$\mathcal{J}^{P_1P_2}(P,q,l)+\mathcal{J}^{P_1P_1}(P,q,l) = -2^{1+2\varepsilon}(-1-i\epsilon)^{-1/2-\varepsilon}B(1/2,1/2+\varepsilon)\pi^{1-\varepsilon}\Gamma(1+\varepsilon)\frac{g^4\mu^{4\varepsilon}}{(2\pi)^{2D-2}}\left(\frac{P_1^2}{P_1^{+2}}\right)^{\varepsilon}\int_0^1\frac{dx}{x^{1+2\varepsilon}}$$
$$\times\int_0^{\mu}\frac{dk_2^+}{k_2^{+1+2\varepsilon}}\int_{k_2^T<\mu}\frac{d^{D-2}k_2^T}{k_2^{+2}}\frac{\frac{P_1\cdot P_2}{P_1^+P_2^+}+\frac{2}{P_1^+P_2^+}(P_2^+P_1^--P_1^+P_2^-)+2[\frac{P_2^T}{P_2^+}-\frac{P_1^T}{P_1^+}]\cdot\frac{P_1^T}{P_1^+}}{[(\frac{k_2^T}{k_2^+}-\frac{P_1^T}{P_1^+})^2+\frac{P_1^2}{P_1^{+2}}]^{1+2\varepsilon}[(\frac{k_2^T}{k_2^+}-\frac{P_2^T}{P_2^+})^2+\frac{P_2^2}{P_2^{+2}}]}$$
$$-(P_2\to P_1). \quad (33)$$

The leading behavior of this expression is a purely imaginary double pole in ε, from the lower limits of the x and k_2^+ integrals. The remaining transverse integration is both infrared and ultraviolet finite, and real, for $\varepsilon\to0$, so that an expansion in ε of this integral can give rise to only imaginary single poles, which vanish in the cross section. The overall factor of $(-1-i\epsilon)^{-\varepsilon}$, however, can convert an imaginary double pole to a *real*, single infrared pole. To isolate the residue of this pole, we need only evaluate the k_2^T transverse integral at $\varepsilon=0$. An important point is that, because we are interested only in noncanceling infrared poles, we may extend the upper limit of the k_2^T integral to infinity. We can do this because, at finite $k_2^T>\mu$, only the k_1 line can produce an infrared pole, at one loop. But, as discussed in [9], for example, all one-loop infrared divergences factorize in the sense of NRQCD.

A simple change of variables, $y_T=k_2^T/k_2^+$, simplifies the transverse integration, evaluated at $\varepsilon=0$ as just described,

$$\int\frac{d^2k_2^T}{(k_2^+)^2}\frac{1}{[(\frac{k_2^T}{k_2^+}-\frac{P_1^T}{P_1^+})^2+\frac{P_1^2}{P_1^{+2}}][(\frac{k_2^T}{k_2^+}-\frac{P_2^T}{P_2^+})^2+\frac{P_2^2}{P_2^{+2}}]}$$
$$=\left(\frac{P_1^{+2}}{P_1^2}\right)\int d^2y_T\frac{1}{[y_T^2+1][(y_T+a_T)^2+\frac{P_2^2}{P_2^{+2}}\frac{P_1^{+2}}{P_1^2}]}, \quad (34)$$

where we define

$$a_T \equiv \left(\frac{P_1^T}{P_1^+} - \frac{P_2^T}{P_2^+}\right)\sqrt{\frac{P_1^{+2}}{P_1^2}}. \tag{35}$$

Next, introducing another Feynman parametrization, w, for y_T and integrating over y_T we get

$$\int d^2y_T \frac{1}{[y_T^2+1][(y_T+a_T)^2 + \frac{P_2^2}{P_2^{+2}}\frac{P_1^{+2}}{P_1^2}]} = \pi\int_0^1 dw \frac{1}{[1-w-w^2a_T^2 + w(a_T^2 + \frac{P_2^2}{P_2^{+2}}\frac{P_1^{+2}}{P_1^2})]}. \tag{36}$$

After integrating over w we then find, for the original k_2^T integral,

$$\int \frac{d^2k_2^T}{(k_2^+)^2} \frac{1}{[(\frac{k_2^T}{k_2^+} - \frac{P_1^T}{P_1^+})^2 + \frac{P_1^2}{P_1^{+2}}][(\frac{k_2^T}{k_2^+} - \frac{P_2^T}{P_2^+})^2 + \frac{P_2^2}{P_2^{+2}}]} = \frac{\pi}{c}\ln\left[\frac{a+c}{a-c}\right], \tag{37}$$

where

$$a \equiv \frac{2P_1\cdot P_2}{P_1^+P_2^+} \qquad c \equiv a\sqrt{1-\frac{P_1^2P_2^2}{(P_1\cdot P_2)^2}}. \tag{38}$$

We are now ready to isolate the real single pole, as indicated above. The poles of the remaining x and k_2^+ integrations in Eq. (33) are found by using $1/f^{1+a} = -\delta(f)/a$, and for the ε-dependent phase, the expansion

$$(-1 \pm i\epsilon)^\varepsilon = e^{\pm i\pi\varepsilon} = 1 \pm i\pi\varepsilon + \mathcal{O}(\varepsilon^2) + \ldots \tag{39}$$

gives the corresponding ε term. We then find from Eq. (33), adding the two remaining diagrams (which are determined by simple substitution),

$$2\,\mathrm{Re}[\mathcal{J}^{P_1P_2} + \mathcal{J}^{P_2P_1} + \mathcal{J}^{P_1P_1} + \mathcal{J}^{P_2P_2}] = \frac{\alpha_s^2}{4\varepsilon}\left[\left(1 + \frac{P_1^+P_2^+}{P_1\cdot P_2}\Delta P^2\right)\frac{1}{2h}\ln\left(\frac{1+h}{1-h}\right) - 1\right], \tag{40}$$

where ΔP^2 and h depend on the momenta of the pair as

$$\Delta P^2 \equiv \left(\frac{P_1}{P_1^+} - \frac{P_2}{P_2^+}\right)^2, \qquad h \equiv \sqrt{1 - \frac{P_1^2P_2^2}{(P_1\cdot P_2)^2}}. \tag{41}$$

It is easy to see that h is proportional to the velocity of the heavy quarks in the center-of-mass system. We will give an explicit expression for its full v dependence below, after identifying the poles of the $\mathcal{K}$ terms. Taken in isolation, however, the sum of the $\mathcal{J}$ terms is manifestly not independent of the choice of l^μ, because of the explicit dependence on the factors $P_i^+ = P_i\cdot l$ in (40).[4] Independence from the direction of the lightlike Wilson line used to define the underlying matrix element will, however, emerge below, once we find the infrared poles of the $\mathcal{K}$ terms.

D. The IR pole from the $\mathcal{K}$ terms

Now we evaluate the remaining terms in Eq. (30), for which the factor $k_1^+ - k_2^+$ remains in the denominator, such as $\mathcal{K}^{P_1P_2} = \mathcal{I}^{P_1P_2} - \mathcal{J}^{P_1P_2}$. In these cases, the virtual k_1^+ dependence in the denominators is no longer quadratic, and the integral requires a slightly more elaborate approach. Specifically, the contributions from the P_1P_2 and P_1P_1 diagrams are given by

$$\mathcal{K}^{P_1P_2}(P,q,l) + \mathcal{K}^{P_1P_1}(P,q,l) = -\pi^{1-\varepsilon}\Gamma(1+\varepsilon)\frac{g^4\mu^{4\varepsilon}}{(2\pi)^{2D-2}}\int_0^1 dx\int\frac{dk_2^+}{2k_2^+}\int dk_1^+\int d^{D-2}k_2^T\frac{1}{[k_1^+ - k_2^+ - i\epsilon]} \times\frac{1}{[L(P_1) - i\epsilon]^{1+\varepsilon}}\left[\frac{\frac{P_1\cdot P_2}{P_1^+}(2k_2^+) + 2P_2^+[\frac{P_2^T}{P_2^+} - \frac{P_1^T}{P_1^+}]\cdot[G^T(P_1) - k_2^T]}{[\frac{P_2^+k_2^{T2}}{2k_2^+} + P_2^-k_2^+ - P_2^T\cdot k_2^T - i\epsilon]}\right] - (P_2\to P_1), \tag{42}$$

where

$$G^T(P_1) \equiv xk_2^T + (1-x)k_2^+\frac{P_1^T}{P_1^+}. \tag{43}$$

At this stage we employ another Feynman parametrization (y) to organize and perform the k_2^T integration. As for the $\mathcal{J}$ terms, we may extend the upper limit of the transverse integral to infinity, with the result

$$\mathcal{K}^{P_1P_2} + \mathcal{K}^{P_1P_1} = \frac{-1}{32\pi^4}g^4(4\pi\mu^2)^{2\varepsilon}\Gamma(1+2\varepsilon)\int_0^1 dx\int_0^1 dy y^\varepsilon\int dk_1^+\int\frac{dk_2^+}{k_2^+}\frac{k_2^+}{[k_1^+ - k_2^+ - i\epsilon]} \times\left[k_2^+\left(\frac{P_1\cdot P_2}{P_1^+P_2^+} + \Delta P^2(1-x)(1-y)\right)\right]\frac{1}{(M-i\epsilon)^{1+\varepsilon}(N+i\epsilon)^{1+2\varepsilon}} - (P_2\to P_1), \tag{44}$$

where we define

[4] It is interesting to observe that the overall result in (40) is invariant under independent rescalings of P_1, P_2, and l, as expected for the eikonal approximation.

$$M \equiv x\left(\frac{k_1^+}{k_2^+} - x\right),$$
$$N \equiv k_2^{+2}\left[-y(1-y)\Delta P^2 + \frac{y}{x}\left(\frac{k_1^+ P_1^2}{k_2^+ P_1^{+2}} - (x - x/y)\frac{P_2^2}{P_2^{+2}}\right)\right], \tag{45}$$

with ΔP^2 defined in Eq. (41). In Eqs. (42) and (44), we have exhibited $\mathcal{K}^{P_1P_2}$, from the third diagram in Fig. 2(a). The other term may be found as indicated, simply by replacing P_2 everywhere by P_1, which leads to a number of simplifications. For example, ΔP^2 is replaced by zero in these terms.

Equation (44) can be reorganized slightly to yield

$$\mathcal{K}^{P_1P_2} + \mathcal{K}^{P_1P_1} = \frac{-1}{32\pi^4} g^4 (4\pi\mu^2)^{2\varepsilon}\Gamma(1+2\epsilon)\int_0^1 dx \int_0^1 dy y^{\varepsilon} \int_0^{\mu} \frac{dk_2^+}{k_2^{+1+4\varepsilon}} \int_{-\infty}^{\infty} \frac{dz}{z - 1 - i\epsilon}$$
$$\times \frac{1}{(x(z-x) - i\epsilon)^{1+\varepsilon}(y/x)^{1+2\varepsilon}} \frac{1}{[-x(1-y)\Delta P^2 \frac{P_1^{+2}}{P_1^2} + x(1/y-1)\frac{P_1^{+2}}{P_2^{+2}}\frac{P_2^2}{P_1^2} + z + i\epsilon]^{1+2\varepsilon}} \left(\frac{P_1^{+2}}{P_1^2}\right)^{1+2\varepsilon}$$
$$\times \left[\left(\frac{P_1 \cdot P_2}{P_1^+ P_2^+} + \Delta P^2 (1-x)(1-y)\right)\right] - (P_2 \to P_1), \tag{46}$$

where we define $z = k_1^+/k_2^+$. The variable z appears in three denominators, one of which is a simple pole at $z = 1$ in the upper half-plane. To perform the z integral in Eq. (46), we combine the remaining two denominators by introducing another Feynman parameter, y',

$$\frac{1}{(x(z-x) - i\epsilon)^{1+\varepsilon}} \frac{1}{[-x(1-y)\Delta P^2 \frac{P_1^{+2}}{P_1^2} + x(1/y-1)\frac{P_1^{+2}}{P_2^{+2}}\frac{P_2^2}{P_1^2} + z + i\epsilon]^{1+2\varepsilon}}$$
$$= \frac{1}{x^{1+\varepsilon}} \frac{\Gamma(2+3\varepsilon)}{\Gamma(1+\varepsilon)\Gamma(1+2\varepsilon)} \int_0^1 dy' \frac{y'^{\varepsilon}(1-y')^{2\varepsilon}(-1+i\epsilon)^{-1-2\varepsilon}}{[(2y'-1)z + x(1-y')((1-y)\Delta P^2 \frac{P_1^{+2}}{P_1^2} - \frac{1-y}{y}\frac{P_1^{+2}}{P_2^{+2}}\frac{P_2^2}{P_1^2}) - xy' - i\epsilon]^{2+3\varepsilon}}. \tag{47}$$

Notice that, before the combination of these two z-dependent denominators with fractional powers, we factor $-1 + i\epsilon$ from the second of the two, so that the $i\epsilon$ on the right-hand side of (47) has a definite sign: $-i\epsilon$. It is perhaps worth noting further how we determine this prescription. As z varies from $-\infty$ to $+\infty$, the second (and first) denominator in (47) can vanish, but for any variable denominator, denoted W, we have

$$W + i\epsilon = W \quad \text{if } W > 0, \qquad W + i\epsilon = (-1 + i\epsilon)(-W - i\epsilon) \quad \text{if } W < 0. \tag{48}$$

The factor $(-1 + i\epsilon)^{\varepsilon} = 1 + i\pi\varepsilon + \ldots$ in this expression will be particularly important in the calculation below, because as above it will convert an imaginary double pole in ε to a real single pole.

Although Eq. (47) is a bit complicated overall, the combined denominator on the right-hand side gives a branch cut in the z plane that is in the lower (upper) half-plane for $0 < y' < 1/2$ ($1/2 < y' < 1$). Inserting the expression in Eq. (47) back into Eq. (44), we then easily perform the z integral. For $y' > 1/2$ we can complete the z contour in the lower half-plane without enclosing any singularities, and the z integral vanishes. For $y' < 1/2$ we close in the upper half-plane and pick up the simple pole at $z = 1$.

The result of this procedure is

$$\mathcal{K}^{P_1P_2} + \mathcal{K}^{P_1P_1} = \frac{-i(-1-i\epsilon)^{-1-\varepsilon}}{16\pi^3} \frac{\Gamma(2+3\varepsilon)}{\Gamma(1+\varepsilon)} g^4 (4\pi\mu^2)^{2\varepsilon} \int \frac{dk_2^+}{k_2^{+1+4\varepsilon}} \int_0^1 dx x^{\varepsilon} \int_0^1 dy y^{1+2\varepsilon} \int_0^{1/2} dy' y'^{\varepsilon}(1-y')^{2\varepsilon}$$
$$\times \left(\frac{P_1^{+2}}{P_1^2}\right)^{1+2\varepsilon}\left[\frac{P_1 \cdot P_2}{P_1^+ P_2^+} + \Delta P^2 (1-x)(1-y)\right]$$
$$\times \frac{1}{[(1-2y')y + x(1-y)(1-y')f(P_1,P_2) + xyy' + i\epsilon]^{2+3\varepsilon}} - (P_2 \to P_1), \tag{49}$$

where

$$f(P_1, P_2) = \frac{P_1^{+2}}{P_2^{+2}}\frac{P_2^2}{P_1^2} - y\Delta P^2 \frac{P_1^{+2}}{P_1^2}. \tag{50}$$

In the above equation, $(-1 - i\epsilon)^{-1-\varepsilon}$ is obtained by multiplying the overall factor $(-1 + i\epsilon)^{-1-2\varepsilon}$, from Eq. (47), together with $(-1 - i\epsilon)^{-2-3\varepsilon}$, from the denominator on the right-hand side of (49), after the z integration. Although the result has the same number of integrations, the infrared

behavior of the y' integral is straightforward to analyze, which will simplify our determination of the infrared poles.

We can check the infrared behavior of the y' integration by expanding in ε,

$$y'^{\varepsilon}(1-y')^{2\varepsilon} = 1 + \varepsilon[\ln y' + 2\ln(1-y')] + \ldots. \quad (51)$$

The term in square brackets is finite at the end point $y' = 1/2$. Because the denominator is finite at $y' = 0$, the behavior at $y' = 0$ is then no worse than logarithmic, $\int_0^{1/2} dy' \ln y'$, and the y' integral is finite and real for $\varepsilon = 0$. Thus, to identify the real infrared pole, we can replace $y'^{\varepsilon}(1-y')^{2\varepsilon}$ by unity and integrate over y' in (49) to obtain an expression that includes the entire real single pole,

$$\mathcal{K}^{P_1P_2} + \mathcal{K}^{P_1P_1} = i(-1-i\epsilon)^{-1-\varepsilon}\frac{\Gamma(1+3\varepsilon)}{\Gamma(1+\varepsilon)}\frac{1}{16\pi^3}g^4(4\pi\mu^2)^{2\varepsilon}\int\frac{dk_2^+}{k_2^{+1+4\varepsilon}}\int_0^1 dx x^{\varepsilon}$$
$$\times\int_0^1 dy y^{1+2\varepsilon}\frac{P_1^{+2}}{P_1^2}\left(\frac{P_1\cdot P_2}{P_1^+P_2^+}+\Delta P^2(1-x)(1-y)\right)\frac{1}{[-2y-x(1-y)f(P_1,P_2)+xy]}$$
$$\times\left[\frac{1}{[\frac{1}{2}x(1-y)f(P_1,P_2)+\frac{1}{2}xy]^{1+3\varepsilon}}-\frac{1}{[y+x(1-y)f(P_1,P_2)]^{1+3\varepsilon}}\right]-(P_2\to P_1). \quad (52)$$

Here we note that terms of order ε from the y integration can also produce, at worst, imaginary single poles in ε.

The steps that isolate the real infrared pole for the $\mathcal{K}$'s follow the procedure of the previous subsection. The x and y integrals in Eq. (52) are real, and we must identify a $1/\varepsilon$ pole from these. The resulting double pole then combines with the $i\pi\varepsilon$ term from the expansion of the prefactor $(-1-i\epsilon)^{-1-\varepsilon}$ to give a real pole term that survives in the full sum of diagrams.

It is easy to check that the x and y integrals of the second fraction in square brackets in Eq. (52) are both real and finite for $\varepsilon \to 0$. We may thus limit our analysis to the first fraction, which is proportional to $1/x^{1+3\varepsilon}$. The $x \to 0$ limit thus generates another infrared pole, which can be isolated by using the distribution identity, $1/x^{1+a} = -\delta(x)/a$, while the y integral can be performed at $\varepsilon = 0$.

For the remaining analysis, it is convenient to combine Eq. (52) with the corresponding results from the other two diagrams in Fig. 2(a), which can be found by substitution. After performing the x integration in (52) we obtain, suppressing the finite part,

$$\mathcal{K}^{P_1P_2} + \mathcal{K}^{P_2P_1} + \mathcal{K}^{P_1P_1} + \mathcal{K}^{P_2P_2}$$
$$= \frac{i(-1-i\epsilon)^{-1-\varepsilon}}{32\pi^3\varepsilon}\frac{\Gamma(1+3\varepsilon)}{\Gamma(1+\varepsilon)}2^{3\varepsilon}g^4(4\pi\mu^2)^{2\varepsilon}$$
$$\times\int_0^{\mu}\frac{dk_2^+}{k_2^{+1+4\varepsilon}}\int_0^1 dy y^{2\varepsilon}\left(\frac{P_1^{+2}}{P_1^2}\right)^{1+2\varepsilon}\left[\frac{P_1\cdot P_2}{P_1^+P_2^+}\right.$$
$$\left.+\Delta P^2(1-y)\right]\frac{1}{[y+(1-y)f(P_1,P_2)]^{1+3\varepsilon}}$$
$$+(P_1\leftrightarrow P_2)-(P_2\to P_1)-(P_1\to P_2). \quad (53)$$

Taking into account the k_2^+ integral, we see that this expression has an overall imaginary double pole which, however, cancels when the complex conjugate diagrams are combined.

The leading, *real* pole in ε can be obtained from the above equation by setting $\varepsilon \to 0$ in the y integral, which then reduces to the sum of two elementary integrations. The first has a y-independent numerator in the integrand,

$$\int_0^1 dy\frac{P_1^{+2}/P_1^2}{[y+(1-y)f(P_1,P_2)]}$$
$$=\int_0^1 dy\frac{P_2^{+2}/P_2^2}{[y+(1-y)f(P_2,P_1)]}=\frac{1}{c}\ln\left[\frac{a+c}{a-c}\right], \quad (54)$$

with a and c defined in Eq. (38). The additional term is linear in y in the numerator, and is given by

$$\int_0^1 dyy\frac{P_1^{+2}/P_1^2}{[y+(1-y)f(P_1,P_2)]}$$
$$=\frac{d(P_1,P_2)}{2c}\ln\left[\frac{a+c}{a-c}\right]+\frac{1}{2\Delta P^2}\ln\left[\frac{P_1^2P_2^{+2}}{P_2^2P_1^{+2}}\right], \quad (55)$$

where a and c are defined in (38), ΔP^2 in (41), and

$$d(P_1,P_2)\equiv 1-\frac{1}{\Delta P^2}\left(\frac{P_1^2}{P_1^{+2}}-\frac{P_2^2}{P_2^{+2}}\right). \quad (56)$$

Although the integral of Eq. (55) is not symmetric in P_1 and P_2, once we add the four diagrams we obtain symmetric results, equal to (54),

$$\int_0^1 dyy\left[\frac{P_1^{+2}/P_1^2}{y+(1-y)f(P_1,P_2)}+\frac{P_2^{+2}/P_2^2}{y+(1-y)f(P_2,P_1)}\right]$$
$$=\frac{1}{c}\ln\left[\frac{a+c}{a-c}\right]. \quad (57)$$

Combining the results above in Eq. (53), and using

$$(-1\pm i\epsilon)^{\varepsilon}=e^{\pm i\pi\varepsilon}=1\pm i\pi\varepsilon+\mathcal{O}(\varepsilon^2)+\ldots, \quad (58)$$

we obtain for the infrared pole

$$2\,\mathrm{Re}[\mathcal{K}^{P_1P_2} + \mathcal{K}^{P_2P_1} + \mathcal{K}^{P_1P_1} + \mathcal{K}^{P_2P_2}]$$
$$= \frac{\alpha_s^2}{4\varepsilon}\left[2 - \left(\frac{2P_1\cdot P_2}{P_1^+P_2^+} + \Delta P^2\right)\frac{1}{c}\ln\left(\frac{a+c}{a-c}\right)\right]$$
$$= \frac{\alpha_s^2}{4\varepsilon}\left[2 - \left(2 + \frac{P_1^+P_2^+}{P_1\cdot P_2}\Delta P^2\right)\frac{1}{2h}\ln\left(\frac{1+h}{1-h}\right)\right], \quad (59)$$

with h defined in Eq. (41). Again, we find a dependence on the choice of vector l, which, however, cancels in the sum of the $\mathcal{J}$'s and $\mathcal{K}$'s.

E. The IR pole in $\mathcal{I}^{8\to1}$

Now adding Eqs. (40) and (59) we find from Eq. (30)

$$\mathcal{I}^{(8\to1)} = 2\,\mathrm{Re}[\mathcal{I}^{P_1P_2} + \mathcal{I}^{P_2P_1} + \mathcal{I}^{P_1P_1} + \mathcal{I}^{P_2P_2}]$$
$$= \frac{\alpha_s^2}{4\varepsilon}\left[1 - \frac{1}{2h}\ln\left(\frac{1+h}{1-h}\right)\right], \quad (60)$$

with the function h defined in Eq. (41). This is the general expression for the pole part of $\mathcal{I}^{(8\to1)}$. A short calculation shows that the lowest-order expansion of Eq. (60) reproduces the result of Ref. [9], Eq. (15) given above for the infrared pole at order v^2 (electric dipole). As anticipated above, our result is independent of the direction of the lightlike vector l^μ that defines the integrals.

To derive an equivalent form in terms of the relative velocity, we use $P = P_1 + P_2$ and $2q = P_1 - P_2$ and recall that we identify the relative velocity with the heavy quark velocity in the center of mass of the pair: $\vec{v} = \vec{q}/E^*$, where $2E^*$ is the total energy of the heavy quark pair in this frame. In these terms, we may replace the quantity h of Eq. (60) with an explicit function of velocity,

$$\mathcal{I}^{(8\to1)} = \frac{\alpha_s^2}{4\varepsilon}\left[1 - \frac{1}{2f(|\vec{v}|)}\ln\left[\frac{1+f(|\vec{v}|)}{1-f(|\vec{v}|)}\right]\right], \quad (61)$$

where with $v = |\vec{v}|$, the function $f(v)$ is given by

$$f(v) = \frac{2v}{1+v^2}. \quad (62)$$

Equation (61) is the general result at NNLO for the infrared pole. As Eqs. (61) and (62) show, the infrared term is independent of the eikonal momentum l for finite v. Hence the infrared pole structure at NNLO in α_s is consistent with factorization, which at this order in α_s is valid to all orders in the relative velocity v in the heavy quarkonium system.

IV. CONCLUSIONS

Equations (61) and (62) provide a remarkably compact expression for the single pole in the infrared factor $\mathcal{I}^{(8\to1)}$ of Eq. (12) at NNLO for finite relative velocity v, or equivalently, expanded to all orders in v. This result is independent of the direction l^μ of the octet Wilson line, and hence is consistent with NRQCD factorization, as discussed in connection with Eq. (8). As shown in Ref. [9], the absence of l dependence in gauge-completed matrix elements enables them to match all NNLO infrared divergent corrections to multijet cross sections. All the arguments in that reference for matching at order v^2 apply here to all orders in v.

Although limited to NNLO, our result suggests that the decoupling of light parton dynamics from heavy quark pair production is robust in perturbation theory at the level of infrared divergences. Evidently, at NNLO, while a lightlike, energetic parton can resolve the color structure of a heavy quark pair, it does so in a way that is independent of the direction of the relative motion of the pair. This suggests to us that the results derived here may generalize to higher orders in soft gluon exchange.

In closing we note that there are, of course, many terms in a general NRQCD velocity expansion that are not given by the eikonal approximation, in particular, those that deal with spin. The eikonal approximation, however, does reproduce infrared divergences as they appear in perturbative calculations of heavy quark production. Clearly, an extension of this analysis to higher orders in the coupling will be of interest.

ACKNOWLEDGMENTS

This work was supported in part by the National Science Foundation, Grant No. PHY-0354776 and No. PHY-0354822, and in part by the US Department of Energy under Grant No. DE-FG02-87ER-40371.

[1] G. T. Bodwin, E. Braaten, and G. P. Lepage, Phys. Rev. D **51**, 1125 (1995); **55**, 5853(E) (1997).

[2] E. Braaten and S. Fleming, Phys. Rev. Lett. **74**, 3327 (1995); P. L. Cho and A. K. Leibovich, Phys. Rev. D **54**, 6690 (1996); **53**, 6203 (1996); E. Braaten, S. Fleming, and A. K. Leibovich, Phys. Rev. D **63**, 094006 (2001); M. Krämer, Prog. Part. Nucl. Phys. **47**, 141 (2001); M. Klasen, B. A. Kniehl, L. N. Mihaila, and M. Steinhauser, Phys. Rev. Lett. **89**, 032001 (2002); G. C. Nayak, M. X. Liu, and F. Cooper, Phys. Rev. D **68**, 034003 (2003); F. Cooper, M. X. Liu, and G. C. Nayak, Phys. Rev. Lett. **93**, 171801 (2004).

[3] M. Beneke and I. Z. Rothstein, Phys. Rev. D **54**, 2005 (1996); **54**, 7082(E) (1996); W. K. Tang and M. Vanttinen, Phys. Rev. D **54**, 4349 (1996); S. Gupta and K. Sridhar, Phys. Rev. D **54**, 5545 (1996); **55**, 2650 (1997).

[4] A. A. Affolder *et al.* (CDF Collaboration), Phys. Rev. Lett. **85**, 2886 (2000); P. L. Cho and M. B. Wise, Phys. Lett. B **346**, 129 (1995); E. Braaten, B. A. Kniehl, and J. Lee, Phys. Rev. D **62**, 094005 (2000); E. Braaten and J. Lee, Phys. Rev. D **63**, 071501 (2001); M. Beneke and M. Kramer, Phys. Rev. D **55**, R5269 (1997); A. K. Leibovich, Phys. Rev. D **56**, 4412 (1997); M. Beneke and I. Z. Rothstein, Phys. Lett. B **372**, 157 (1996); **389**, 769(E) (1996).

[5] K. Abe *et al.* (Belle Collaboration), Phys. Rev. Lett. **89**, 142001 (2002); B. Aubert *et al.* (*BABAR* Collaboration), Phys. Rev. D **72**, 031101 (2005).

[6] F. Cooper, E. Mottola, and G. C. Nayak, Phys. Lett. B **555**, 181 (2003); G. C. Nayak, A. Dumitru, L. D. McLerran, and W. Greiner, Nucl. Phys. **A687**, 457 (2001); X. N. Wang, Phys. Rep. **280**, 287 (1997); X. M. Xu, D. Kharzeev, H. Satz, and X. N. Wang, Phys. Rev. C 53, 3051 (1996); G. C. Nayak, J. High Energy Phys. 02 (1998) 005.

[7] D. Acosta *et al.* (CDF Collaboration), Phys. Rev. D **71**, 032001 (2005); V. M. Abazov *et al.* (D0 Collaboration), Phys. Rev. Lett. **94**, 232001 (2005).

[8] N. Brambilla *et al.*, hep-ph/0412158; M. Bedjidian *et al.*, hep-ph/0311048; G. T. Bodwin, Int. J. Mod. Phys. A **21**, 785 (2006); J. P. Lansberg, Int. J. Mod. Phys. A **21**, 3857 (2006).

[9] G. C. Nayak, J. W. Qiu, and G. Sterman, Phys. Lett. B **613**, 45 (2005); Phys. Rev. D **72**, 114012 (2005); hep-ph/0512345.

[10] E. Braaten, S. Fleming, and T. C. Yuan, Annu. Rev. Nucl. Part. Sci. **46**, 197 (1996).